AIAA JOURNAL
Vol. 44, No. 10, October 2006

Scaling Laws and a Method for Identifying Components of Jet Noise

K. Viswanathan*
The Boeing Company, Seattle, Washington

DOI: 10.2514/1.18486

It is well established that there are three principal jet noise components for imperfectly expanded supersonic jets. However, to this date there has been no reliable and practical method for identifying the individual components. First, new scaling laws for the turbulent mixing noise component are developed from a comprehensive experimental database generated by the author. The scaling laws are based on the explicit recognition that a) the variation of the overall sound power level with jet velocity has a weak dependence on jet stagnation temperature ratio; b) the variation of the overall sound pressure level with velocity at every radiation angle is a function of jet stagnation temperature ratio. Therefore, the behavior of the turbulent mixing noise at each radiation angle can be characterized by the two independent parameters: the velocity ratio and the stagnation temperature ratio. These two findings set this study apart from past approaches and form the basis for the methodology developed here. It is demonstrated clearly that there is excellent collapse of the mixing noise spectra over the entire frequency range. Once the normalized or master spectra for the mixing noise are established, it is a trivial matter to subtract these from the total measured spectra to obtain the shock-associated noise. For moderately imperfectly expanded heated supersonic jets, the mixing noise component has the same spectral level as the shock-associated noise, over a wide range of higher frequencies. At the lower radiation angles in the forward quadrant, there is a substantial decrease in the values of the velocity exponents as the stagnation temperature ratio is increased. Proceeding aft, the values start to rise and in the peak sector of noise radiation, the velocity exponent becomes less sensitive to jet stagnation temperature ratio unlike at lower angles, and stays close to the values for the unheated jet.

I. Introduction

IT is well established that there are three principal noise components for an imperfectly expanded supersonic jet. These are the turbulent mixing noise, the broadband shock-associated noise, and the screech tones. A convergent nozzle operated at supercritical pressure ratios always produces shocks in the plume, resulting in shock-associated noise. The same situation prevails when a convergent-divergent nozzle is operated at off-design conditions. The intensity of shock-associated noise is dependent on the degree of mismatch between the design Mach number (M_d) and the fully expanded jet Mach number (M_j). The relative importance of the broadband shock-associated noise and turbulent mixing noise is a strong function of radiation angle and jet operating conditions. The shock noise radiation is omnidirectional, while the mixing noise is radiated principally to the aft directions.

Harper-Bourne and Fisher [1] were the first to provide experimental evidence of broadband shock-associated noise. Subsequently, Tanna [2], Seiner and Norum [3,4], Norum and Seiner [5,6], Tam and Tanna [7], Seiner [8], Seiner and Yu [9] and Yamamoto et al. [10] carried out extensive studies that have formed the basis for our understanding of shock-associated noise. The experiments at NASA Langley by Seiner, Norum, and Yu concentrated on the aerodynamic characteristics, near field acoustics and far field acoustics of shock-containing plumes in order to uncover the physical mechanisms responsible for the generation of shock noise. The main characteristics of shock-associated noise, summarized above, resulted from these experimental investigations. The physical mechanisms responsible for the generation of this component of noise were explained by the theory of Tam and Tanna [7], and Tam [11,12]. A prediction method based on this theory was shown to capture the experimentally observed characteristics very well.

The characteristics of turbulent mixing noise have been examined since the late 1940s and early 1950s. Many studies (too numerous to cite here), both theoretical and experimental, have been carried out since that time. In spite of all these efforts, there is no theory or methodology that can predict the spectral characteristics at all the radiation angles from a simple round jet. Given this situation, empirical noise prediction schemes are used both for single and dual-stream jets. The most common one is the SAE [13] method. Though these methods provide reasonable predictions over a wide range of jet velocities and operating conditions, the agreement with data at any particular condition could be poor and hence may not be within acceptable accuracy limits. Perhaps it should not be surprising then that there is no validated methodology for identifying the component of turbulent mixing noise in jet noise spectra from supersonic jets that contain broadband shock-associated noise as well.

The objectives of the current study are as follows: new scaling laws for the turbulent mixing noise component are first developed. Two practical applications are then described. These scaling laws are utilized for identifying the mixing noise component in spectra that contain both the mixing noise and the broadband shock-associated noise. This approach does not depend on any prediction method and is based entirely on an experimental database. The validity of this method is demonstrated for a variety of test cases from shock-containing jets at various pressure and stagnation temperature ratios, and the robustness of the approach is established. It is also highlighted that a practical and accurate noise prediction methodology is a natural by-product of the current approach. This prediction methodology, another useful outcome of the scaling laws, is described elsewhere.

II. Experimental Database

A comprehensive aeroacoustic database, from unheated and heated jets over a wide range of Mach numbers and stagnation temperature ratios, has been developed using axisymmetric nozzles of different diameters. Several issues that could have an impact on the radiated noise, such as the effect of the Reynolds number, the effect of the state of the flow (laminar or turbulent) at the nozzle exit, the effect of jet temperature, the effect of jet density for jets at constant

Presented as Paper 2935 at the 11th AIAA/CEAS Aeroacoustics Conference, Monterey, CA, 23–25 May 2005; received 29 June 2005; revision received 18 February 2006; accepted for publication 27 February 2006.

*MS 67-ML, P.O. Box 3707, Seattle, WA 98124-2207; k.viswanathan@boeing.com. Associate Fellow AIAA.

velocity, the effect of nozzle size on data quality, etc., have been investigated and reported in Viswanathan [14–16]. Detailed descriptions of the test facility, the jet simulator, the data acquisition and reduction process, etc., may be found in Viswanathan [14]. For the sake of completeness, a brief overview is provided here. The jet simulator is embedded in an open-jet wind tunnel, which can provide a maximum free-stream Mach number of 0.32. The takeoff Mach numbers for all commercial aircraft fall in the range of 0.24 to 0.28; hence, the effects of forward flight can be evaluated at realistic free-stream velocities in Boeing's Low Speed Aeroacoustic Facility. Bruel & Kjaer quarter-inch Type 4939 microphones are used for free-field measurements. The microphones are set at normal incidence and without the protective grid, which yields a flat frequency response up to 100 KHz. Typically, several linear microphone arrays are used. The microphones in each array are laid out at a constant sideline distance of 15 ft (4.572 m) from the jet axis. Very fine narrow band data with a bin spacing of 23.4 Hz up to a maximum frequency of 88, 320 Hz are acquired and synthesized to produce one-third octave spectra, with a center band frequency range of 200 to 80,000 Hz.

Aeroacoustic data have been acquired at five stagnation temperature ratios (T_t/T_a) of 1.0, 1.8, 2.2, 2.7, and 3.2. Throughout this paper, the stagnation or total temperature ratio is quoted. Unless otherwise stated, the terminology "jet temperature ratio" denotes the stagnation temperature ratio. At each jet temperature, the nozzle pressure ratio (NPR) was varied systematically so as to produce jets with Mach numbers of 0.3, 0.4, 0.5, 0.6, 0.7, 0.8, 0.9, 1.0, 1.24, 1.36, 1.47, and 1.58. Thus, at each fixed temperature ratio, data were acquired over a wide range of jet velocities. It is well known that the jet velocity (or the velocity normalized by the ambient speed of sound V_j/a) is a key parameter in turbulent mixing noise. The above test matrix, by no means unique but convenient nonetheless, provides the requisite range of jet velocities at each specified temperature ratio that would permit the development of scaling laws. Apart from this main test matrix, data were taken at other jet conditions as well. Nozzles of different diameters have also been used to acquire data at the above jet conditions. It is worth mentioning another significant and beneficial attribute of this database. It was demonstrated clearly in Viswanathan [14,15] that the noise data are of the highest quality over the entire frequency range. It was pointed out that the spectral measurements at the higher frequencies were severely contaminated in most facilities, thereby rendering them unsuitable for scientific applications. Consequently, existing empirical prediction methods based on these data are suspect. Many concerns with the instrumentation system and the proper steps that would lead to accurate measurements at the higher frequencies are discussed by Viswanathan [17]. The use of larger nozzles and accurate measurements up to 80 KHz, have extended the Strouhal number range considerably in the current database. The salient characteristics of heated and unheated jets at subsonic Mach numbers were reported in Viswanathan [15]. The entire database is utilized in the current paper.

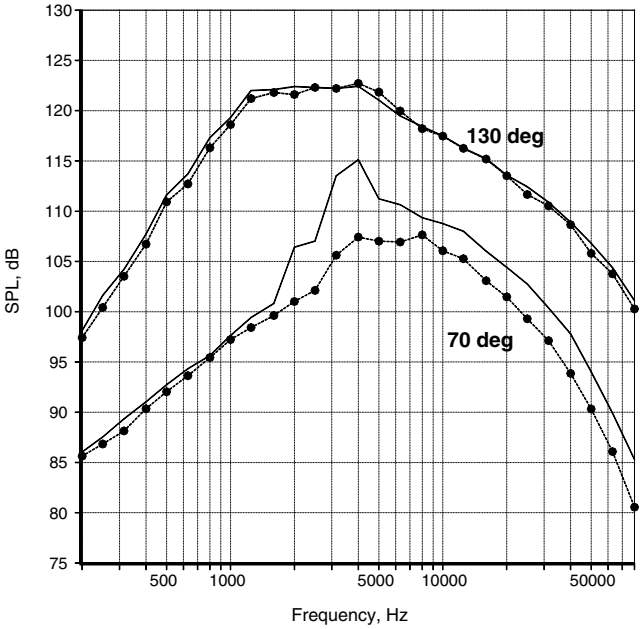

Fig. 1 Comparison of spectra at 70 and 130 deg from a supersonic jet. $M_j = M_d = 1.36$, $T_t/T_a = 2.78$. Solid lines: convergent nozzle; ● and dashed: CD nozzle.

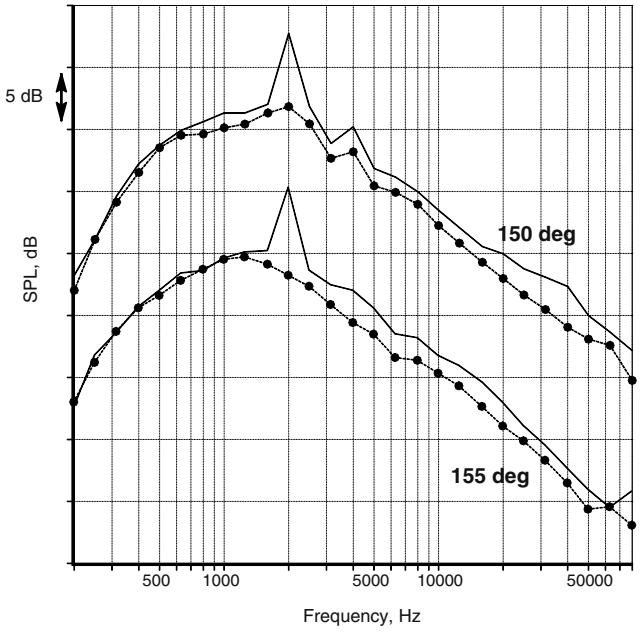

Fig. 2 Comparison of spectra at 150 and 155 deg from a supersonic jet. $M_j = M_d = 1.36$, $T_t/T_a = 2.78$. Solid lines: convergent nozzle; ● and dashed: CD nozzle.

III. Description of the Methodology

A. Characteristics of Mixing and Shock-Associated Noise

Let us first review the characteristics of the turbulent mixing noise and broadband shock-associated noise from a supersonic jet at a Mach number of 1.36 and at a total temperature ratio (T_t/T_a) of 2.78. The spectra measured from a convergent nozzle and a convergent-divergent (CD) nozzle with a design Mach number of 1.36 and at various radiation angles are shown in Figs. 1 and 2. The polar angles quoted here are measured from the jet inlet axis. The data are corrected to a common distance of 20 ft (6.096 m) from the center of the nozzle exit (coordinate system with origin at the center of the nozzle exit) and lossless or standard-day conditions: ambient temperature of 77°F (298 K) and relative humidity of 70%. The atmospheric attenuation coefficients are obtained from the method of Shields and Bass [18]. The standard practice of converting the as-measured data to lossless form and then propagating the spectra to a common distance (of 20 ft) while accounting for the atmospheric absorption at standard-day conditions has been adopted. Implicit in this process is the assumption of linear propagation, with the sound pressure level obeying the $(1/r^2)$ dependence. The normalization process may be written as

$$\mathrm{SPL}_{(20\ \mathrm{feet})} = \mathrm{SPL}_{\mathrm{measured}} - 10\log_{10}\left(\frac{20}{r}\right)^2 + r[\mathrm{AA}_{(\mathrm{test\ day})}] - 20[\mathrm{AA}_{(\mathrm{std\ day})}]$$

where r (ft) is the distance of the microphone from the origin of the coordinate system, [AA] are the atmospheric absorption coefficients (which are frequency dependent) per foot. The above equation provides spectra corrected to standard-day conditions; for lossless data, the last term in this equation is omitted. The accuracy of the

weather corrections and the suitability of the different proposed methods have been evaluated by Viswanathan [19]; it was shown that the method of Shields and Bass [18] was the best at the higher frequencies of interest in model scale tests.

At 70 deg in Fig. 1, the turbulent mixing noise may be identified at the lower frequencies ($f < 1500$ Hz); the contribution of the broadband shock-associated noise from the convergent nozzle is clearly evident at the higher frequencies resulting in minor humps in the spectra near the spectral peak. The CD nozzle, built with a straight divergent section instead of a contour, is seen to produce weak shocks. At an angle of 130 deg the spectral shapes are identical, indicating that the turbulent mixing noise is the dominant component at this angle. Figure 1 also indicates that at the same fully expanded jet Mach number, the turbulent mixing noise from a convergent nozzle is identical to that from a CD nozzle. That is, the presence of shocks in the plume does not alter the turbulent mixing noise much, a trend noted earlier by Seiner [8]. At further aft angles, Fig. 2, we notice some interesting trends. There is a well-pronounced screech tone at 2000 Hz at both angles; a higher harmonic at 4000 Hz may be identified at 150 deg. There is also broadband amplification of the turbulent mixing noise, indicated by the slightly increased levels at the higher frequencies. That is, there could be amplification of the mixing noise when screech tones are present. Similar trends were observed in the experiments of Seiner [8] and may be seen in Figs. 17 and 18 in Tam et al. [20]. For the unheated jets in the NASA Langley experiments, there was a $\sim$3 dB increase in the mixing noise levels at almost all frequencies, both at the lower angles and at the higher angles where the mixing noise peaks. For the highly heated jet shown here, there is amplification only at the higher frequencies because the levels are comparable at all the angles at the lower frequencies. Though the underlying physics for this phenomenon is not known, it should be noted that the mixing noise levels could be higher when strong screech tones are generated.

The above approach, wherein the noise from a convergent nozzle is compared with that from a CD nozzle at its design Mach number, to identify the turbulent mixing noise provides unambiguous results. A similar exercise was carried out by Tam and Tanna [7]. However, it is not practical because one would have to design, build and test numerous CD nozzles. Clearly, a different approach is needed. It is well established that the intensities of the mixing noise and shock-associated noise have very different dependences on jet operating conditions. The overall power level for mixing noise scales with the eighth power of the jet velocity, Lighthill [21]. The intensity of the shock-associated noise, on the other hand, varies as $(M_j^2 - M_d^2)^2$. We exploit these different scaling characteristics of the two components to identify the mixing noise.

B. Review of Existing Formulations

There have been several attempts in the past to collapse spectra from heated and unheated jets; most of these have relied on the acoustic analogy, together with other theoretical considerations. In many of these, scaling laws for jet noise were developed for a radiation angle of 90 deg, where convection and other effects are negligible. We briefly review these first. Fisher et al. [22] proposed the following scaling law for intensity [the term intensity was used loosely to denote the overall sound pressure level (OASPL) in the past studies]:

$$I_{90} \propto A_1\left(\frac{V_j}{a}\right)^8 + B\left(\frac{V_j}{a}\right)^4$$

A_1 and B were functions of the jet temperature ratio in some fashion. V_j is the jet velocity and a is the speed of sound in the ambient medium. Morfey [23] started with Lighthill's equation and invoked a different set of assumptions and proposed the following relation:

$$I_{90} \propto A_1\left(\frac{V_j}{a}\right)^8 + B\left(\frac{V_j}{a}\right)^6$$

Morfey [23] further suggested that the high- and low-frequency portions of the spectra would behave differently and would have different dependences on jet velocity. Lilley [24] derived a wave equation that accounted for convection effects to obtain,

$$I_{90} \propto A_1\left(\frac{V_j}{a}\right)^8 + B\left(\frac{V_j}{a}\right)^6 + C\left(\frac{V_j}{a}\right)^4$$

Again, A_1, B, and C are complex functions of the temperature ratio and the functional forms depended on the assumptions invoked, with several empirical factors introduced. Tanna et al. [25] examined all these formulations and developed master spectra for the contributions from the Reynolds stress and temperature fluctuations and proposed the following functional form:

$$I_{90} \propto A_1\left(\frac{V_j}{a}\right)^{7.5} + B\left(\frac{V_j}{a}\right)^4$$

They further stated that the two sources are not statistically uncorrelated as assumed in Fisher et al., Morfey, and Lilley [22–24] but appeared to be highly correlated. Morfey et al. [26] developed scaling laws based on geometric acoustics and examined the importance of the three assumed sources of monopole (V^4), dipole (V^6), and quadrupole (V^8), and their contributions to the total noise, with and without these sources being coherent. They concluded that the combination of dipole and quadrupole sources with zero coherence best represented the data. Morfey et al. [26] introduced additional empirical constants that varied with temperature ratio that supposedly provided better fit with data. Tam et al. [20] suggested that when the variation of the OASPL at a particular angle with (V_j/a) is considered, a family of parallel straight lines that correspond to each temperature ratio would result. Goldstein [27] derived a variant of the Lilley's equation without introducing additional approximations and represented the sources as the sum of quadrupole and dipole terms. Goldstein [28] derived a different set of linearized inhomogeneous Euler equations that produced quadrupoles and monopoles as the source terms. He also cautioned that no set of equations based on the acoustic analogy can be used for the identification of the noise sources. It is clear then that there are no commonly accepted scaling laws, with different researchers invoking disparate theoretical arguments (and associated assumptions) to support their formulations. Perhaps the most unsatisfactory aspect is the need for the proportionality constants and functional dependences to vary with Strouhal number at a fixed radiation angle.

C. Proposed Scaling Laws

Viswanathan [15] examined the velocity dependence of overall power level (OAPWL) with the acoustic Mach number (V_j/a) at various stagnation temperature ratios; see Sec. 4.4 in this reference. He correctly pointed out that though the overall power seemingly follows the eighth-power law at all jet temperature ratios, an excellent collapse of OAPWL is obtained by grouping the different test points as per their jet stagnation temperature ratios. For the sake of completeness, Figs. 23 and 24 from Viswanathan [15] are reproduced here as Figs. 3 and 4, respectively. When the OAPWL variation with (V_j/a) is examined in this manner in Fig. 4, the velocity exponent is clearly seen to depend on the stagnation temperature ratio. That is, the jet stagnation temperature ratio is an important controlling parameter:

$$\text{Sound power} \propto \left(\frac{V_j}{a}\right)^n, \qquad n = n\left(\frac{T_t}{T_a}\right)$$

Viswanathan [15] also investigated the velocity dependence of the overall sound pressure levels (OASPL) with the acoustic Mach number (V_j/a), at various temperature ratios and at various radiation angles. As with the OAPWL, the OASPL was also shown to depend on the jet temperature ratio; see Figs. 32 and 33 and associated discussion in Viswanathan [15]. Again, the effect of the stagnation temperature ratio on scaling the noise radiated to a particular angle was demonstrated unambiguously. That is,

$$I_\theta \propto \left(\frac{V_j}{a}\right)^n, \qquad n = n\left(\theta, \frac{T_t}{T_a}\right)$$

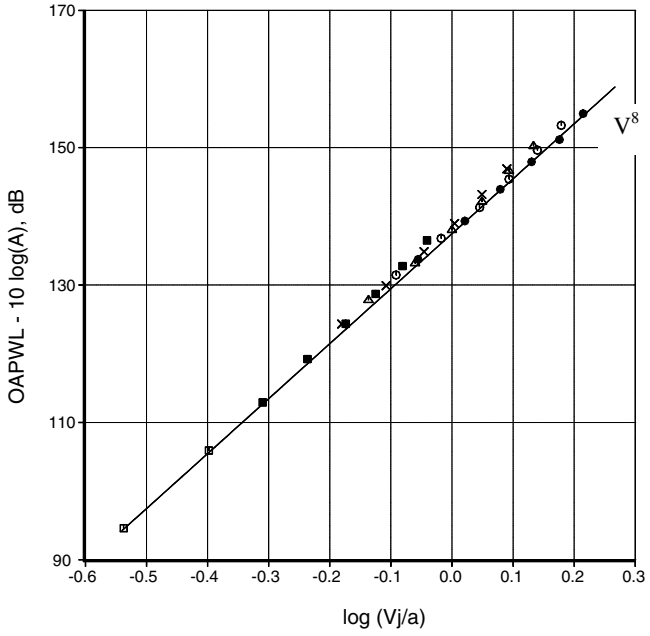

Fig. 3 Variation of OAPWL with jet velocity $D = 2.45$ in. Solid line: V^8. □, ■: $T_t/T_a = 1.0$; ×: $T_t/T_a = 1.8$; △: $T_t/T_a = 2.2$; ○: $T_t/T_a = 2.7$; ●: $T_t/T_a = 3.2$.

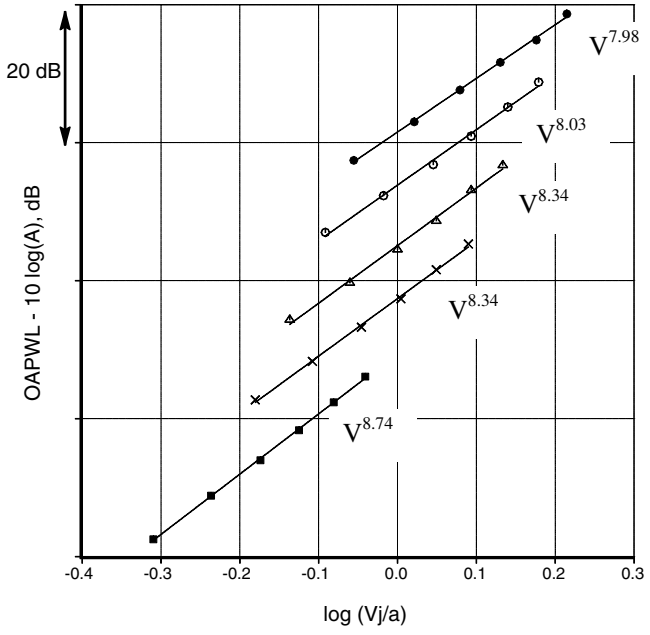

Fig. 4 Variation of OAPWL with jet velocity, $D = 2.45$ in. ■: $T_t/T_a = 1.0$; ×: $T_t/T_a = 1.8$; △: $T_t/T_a = 2.2$; ○: $T_t/T_a = 2.7$; ●: $T_t/T_a = 3.2$.

Note that this relation is valid for all angles (θ) and not just 90 deg. As the jet stagnation temperature ratio is increased progressively, there is a reduction in the velocity exponent in general. Further, the value of the exponent increases as the observer angle is increased from low values to the peak radiation direction in the aft quadrant. It is pointed out that the velocity exponent could be significantly different from eight, see Fig. 16b of Viswanathan [15] for an example. These two important observations, that both the OAPWL and the OASPL at any angle are controlled by the jet stagnation temperature ratio and velocity ratio, are new findings on jet noise and form the underpinning for the approach adopted here. The power of these original observations is demonstrated in the next section.

The various normalization parameters that collapse jet noise spectra were examined in detail in Refs. [15,19]. It was demonstrated clearly that with proper scaling factors for nozzle area and velocity, good collapse of both narrowband and one-third octave spectra are achieved, both for turbulent mixing noise and broadband shock-associated noise. Excellent agreement of spectra acquired at model scale with those at engine scale was demonstrated at all angles and all frequencies for many power settings, both at subsonic and supersonic jet Mach numbers. It was shown conclusively that model data faithfully reproduce engine data, thereby validating the scaling methodology. The application of the methodology is demonstrated with concrete examples in the next section.

IV. Results and Discussion

The effects of jet temperature and jet velocity on the radiated spectra are examined in detail to determine the value of the velocity exponent at each radiation angle. Sample spectra from jets at a fixed jet temperature ratio (T_t/T_a) of 3.2, corrected to a polar distance of 20 ft (6.096 m) and lossless conditions are shown at an angle of 90 deg for a wide range of Mach numbers (0.7–1.58) in Fig. 5. The spectral shapes at the four subsonic Mach numbers are similar; with the correct velocity exponent it should be straightforward to collapse the spectra. For the supersonic Mach numbers, the fully expanded jet diameter is used instead of the geometric or physical diameter of the nozzle. The fully expanded jet diameter for both convergent and CD nozzles for any jet Mach number can be calculated using the formula developed by Tam and Tanna [7]. At the four supersonic Mach numbers, the contribution of the shock-associated noise is clearly evident, with the spectral shapes being very different for Strouhal numbers greater than ~0.4. Before we extract the turbulent mixing noise component at the supersonic Mach numbers, it is worthwhile to reexamine the effect of increasing the jet temperature on noise at fixed supersonic jet Mach numbers.

Figure 6 shows lossless spectra at $M = 1.24$ at the five stagnation temperature ratios of 1.0, 1.8, 2.2, 2.7, and 3.2 at several polar angles. At the lower angles, where the shock-associated noise is dominant, a prominent screech tone is evident whose amplitude is ~25 dB above the broadband noise level for the unheated jet denoted by the black lines. As the jet temperature is increased, the tone level decreases first for $T_t/T_a = 1.8$ (red/light gray lines); at the highest temperature (blue line, top curve) the screech tone is either barely perceptible or has an amplitude of ~5 dB above the broadband levels. In the forward quadrant, there is a near-monotonic increase in levels with increasing jet temperature at the lower frequencies, up to a Strouhal number of ≈0.5. At 60 deg, the broadband shock peaks as well as the

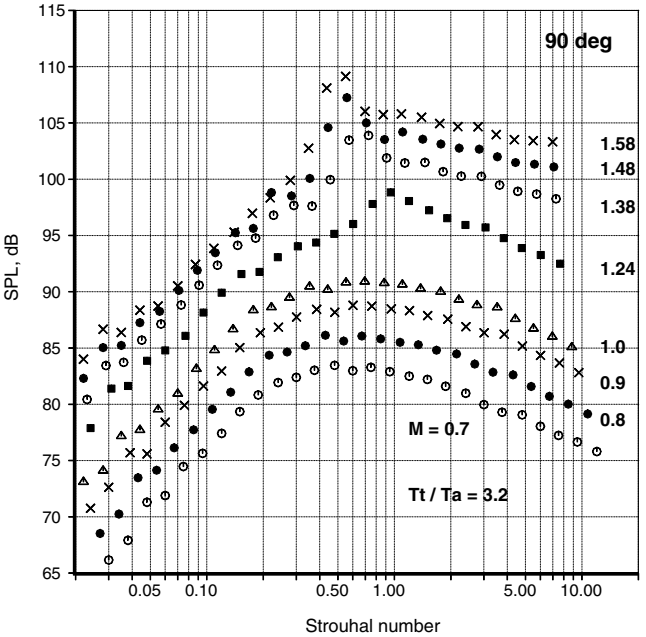

Fig. 5 Measured spectra at 90 deg from heated jets at various Mach numbers. $D = 2.45$ in.; $T_t/T_a = 3.2$.

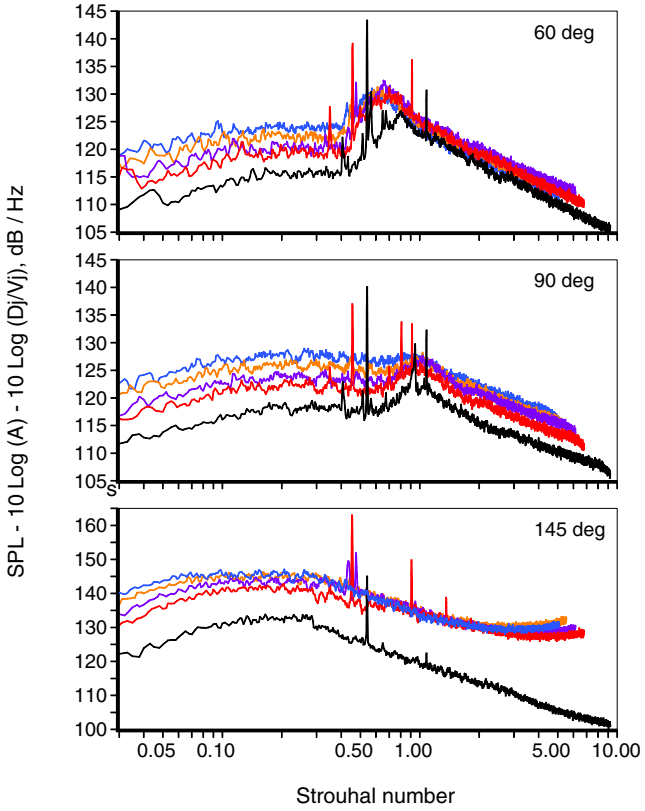

Fig. 6 Effect of jet temperature on supersonic jet noise at different angles. $M = 1.24$, $D = 1.5$ in. Black: $T_t/T_a = 1.0$; red (second from bottom): 1.8; purple (middle): 2.2; orange (second from top): 2.7; blue (top): 3.2.

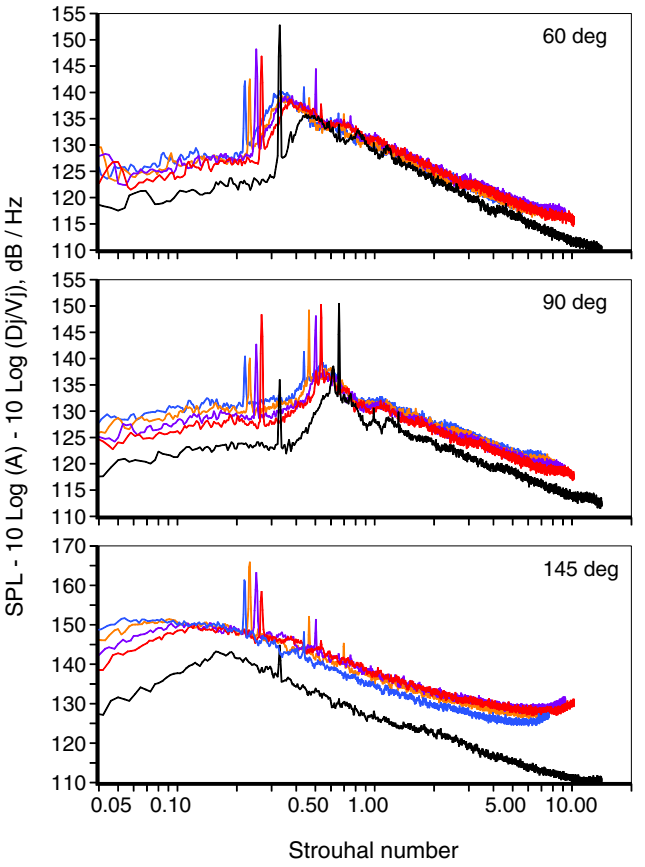

Fig. 7 Effect of jet temperature on supersonic jet noise at different angles. $M = 1.48$, $D = 2.45$ in.. Black: $T_t/T_a = 1.0$; red (second from bottom): 1.8; purple (middle): 2.2; orange (second from top): 2.7; blue (top): 3.2.

screech tones (if present) are clearly evident at higher Strouhal numbers. At still higher Strouhal numbers, there is very little change in spectral levels due to heating. Previous experimental measurements suggest that the turbulent mixing noise component is dominant in the frequency regime where the noise levels increase with jet temperature; the shock-associated noise is dominant at the higher Strouhal numbers where there is very little change in sound pressure levels due to heating. Proceeding downstream, the importance of the mixing noise component becomes more pronounced, until at large aft angles the spectra are totally dominated by the mixing noise, except for the screech tones and any associated amplification of the mixing noise highlighted in Fig. 2. The tail-ups or the flattening of the spectra at the higher frequencies are due to two reasons: the effect of the atmospheric absorption has been removed and the noise from the heated jets is subjected to nonlinear propagation. Viswanathan [19] reported on this unexpected phenomenon and identified a value for jet velocity of ~1600 ft/s (490 m/s) above which there is nonlinear propagation of sound waves, with agglomeration of energy at the higher frequencies. The jet velocities for the heated jets with $M = 1.24$ are 1623 ft/s (495 m/s), 1795 ft/s (547 m/s), 1997 ft/s (609 m/s) and 2179 ft/s (664 m/s), respectively, which are greater than the threshold value. This point is discussed in depth in a future paper on jet noise prediction.

Similar trends are observed at a higher Mach number of 1.48 in Fig. 7. At 60 deg, again there is virtually no change in the spectral levels due to jet temperature above a Strouhal number of ~0.5. At this higher Mach number, screech tones and higher harmonics are observed at all radiation angles even for the heated jets because of the greater mismatch between the nozzle exit pressure and the ambient pressure. Figure 8 shows the effect of jet temperature at a still higher Mach number of 1.58. One-third octave band spectra are shown for a specific reason: in the following results, the mixing and shock-associated components are identified mainly from one-third spectra. A sample case with narrowband spectra is also included to illustrate the approach. Attention is drawn to the fact that depending on the frequency of the screech tone, a single hump that contains both the screech tone and the broadband peak could result if they happen to fall within a particular frequency range that comprises the one-third octave band. Two or more humps may also result as seen at 90 deg, depending on the occurrence of multiple strong harmonics of the fundamental screech tone. Furthermore, the averaging of the energy over ever-increasing bandwidths at the higher frequencies to produce the one-third octave spectra tends to emphasize the spectral levels at the higher frequencies and accentuates the tail-up for the lossless data. Thus, the intent of this figure is to orient the reader to possible spectral shapes observed with one-third octave spectra. It should be noted that both narrowband and one-third octave spectra preserve the same total acoustic energy and are hence equivalent. However, much of the finer resolution seen in the narrowband data is lost when the energy is summed over wide frequency bands.

The turbulent mixing noise for the supersonic cases is identified as follows. The lossless spectra from the subsonic jets at the selected temperature ratio of 3.2 are normalized and the velocity exponents at the radiation angles of 70 and 90 deg are determined to be 5.25 and 5.53, respectively. The parameter $[\mathrm{SPL} - 10^* \log(A) - 10^* n^* \log(V_j/a)]$ is plotted on the y axis for both the subsonic and supersonic Mach numbers in Figs. 9a and 9b, at an angle of 70 deg. (A is the nozzle exit area.) In the above relation, A is dimensional; one could express this area in terms of square inches, square feet, or square meters. Depending on the chosen dimensional unit, the value of the spectral levels would move up or down by a scaling constant. For example, the noise per square foot would be higher than the noise per square inch by 21.58 dB [$10^* \log_{10}(144)$]. However, a consistent use of the same dimensional unit should result in the correct noise levels, regardless of the unit chosen. The dimensional area in square inches is used here. For the supersonic cases, the nozzle exit area is again calculated using the fully expanded jet diameter. In Fig. 9a,

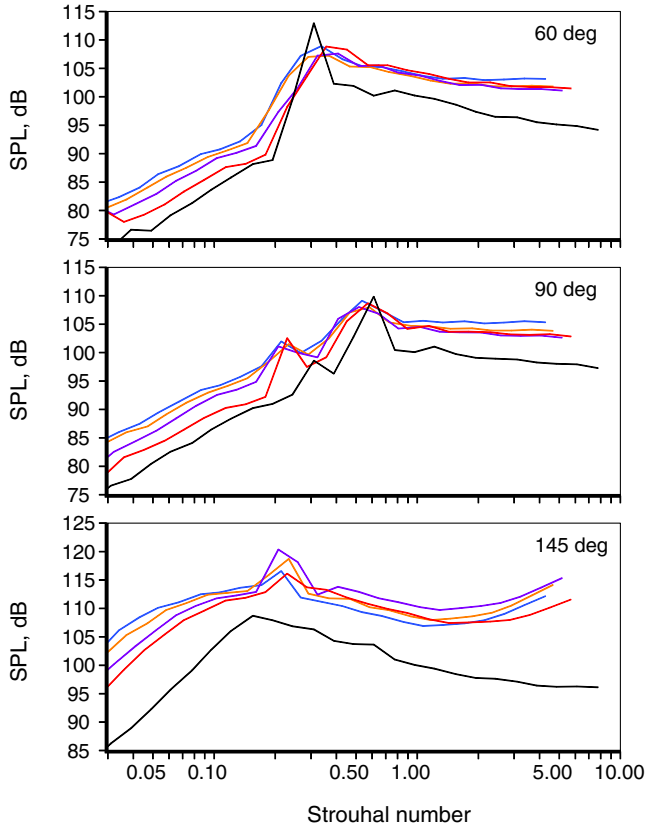

Fig. 8 Effect of jet temperature on supersonic jet noise at different angles. $M = 1.58$, $D = 1.5$ in.. Black: $T_t/T_a = 1.0$; red (second from bottom): 1.8; purple (middle): 2.2; orange (second from top): 2.7; blue (top): 3.2.

one-third octave spectra are shown. There is excellent collapse of the subsonic mixing noise spectra (denoted by the symbols) over the entire frequency (Strouhal number) range. The spectra at the lower Mach numbers (not shown) extend the upper limit of the Strouhal number range, because of lower V_j. This collapse also provides additional confirmation of the excellent data quality; see Sec. IV.E in Viswanathan [17] for a more detailed discussion. We further note that the spectra at supersonic Mach numbers (denoted by lines) agree well with the subsonic ones at the lower frequencies. The cause of the tones at the lower frequencies (at a Strouhal number of ~0.03) was investigated in detail and reported by Viswanathan [14]; these are facility related and are not part of the jet noise. However, no steps have been taken here to remove them. Viswanathan [14] reported on the impact of these tones on noise spectra: these tones were seen at very low angles and were dependent on the mass flow rate and the nozzle pressure ratio. It was clearly demonstrated that these tones do not lead to broadband amplification, see Figs. 24–26 and the discussions on page 1684 in Viswanathan [14]. It is also pointed out that since these tones always appear at fixed frequencies, one can create normalized spectra without tones through a judicious choice of the nozzle diameter and jet velocity. It is clear that the mixing noise component for the supersonic jets is given by the subsonic spectral shape denoted by the symbols.

Figure 9b shows a similar comparison using narrowband spectra; only two subsonic and two supersonic cases are shown for brevity. It is readily apparent that there is excellent collapse of the subsonic spectra (shown by the dark and light gray lines) and that the mixing noise component for the $M = 1.24$ heated jet is denoted by the subsonic spectra. We further note that there is a screech tone at a Strouhal number of ~0.20 for the $M = 1.58$ case, with an amplitude of ~6 dB. An examination of Figs. 9a and 9b indicates that the mixing noise levels at the lower frequencies for the $M = 1.58$ jet is higher by ~1 dB or so. Therefore, it might be necessary to move the mixing noise spectra up by ~1 to ~2 dB for $M = 1.58$. As noted earlier, screech tones could lead to increased levels of mixing noise,

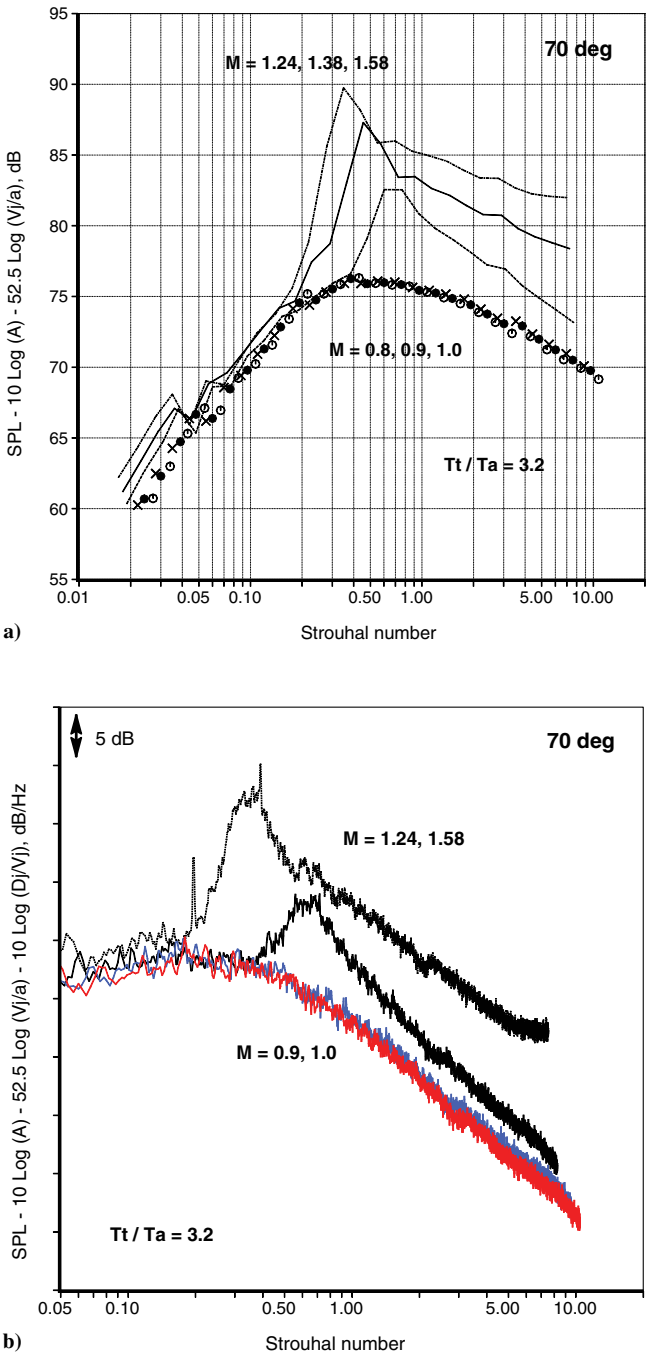

Fig. 9 a) Normalized one-third octave spectra from heated jets at 70 deg. $T_t/T_a = 3.2$, $D = 2.45$ in. Symbols: subsonic Mach numbers; lines: supersonic Mach numbers. Velocity exponent $n = 5.25$. b) Normalized narrowband spectra from heated jets at 70 deg. $T_t/T_a = 3.2$, $D = 2.45$ in. Blue (dark gray) and red (light gray): subsonic Mach numbers; lines: supersonic Mach numbers. Velocity exponent $n = 5.25$.

as seen for the $M = 1.58$ jet. The scaling method shown in Figs. 9a and 9b also provides a measure of the amplification of the turbulent mixing noise due to screech tones. A further conclusion is drawn from these two figures: one may use narrowband or one-third octave data in scaling spectra, also see Viswanathan [19]. The shock-associated component can now be obtained by logarithmically subtracting the mixing noise component from the total measured noise.

In the literature, it is mentioned that the mixing noise component is "to the left of the broadband shock peak or the screech tone, mainly at the lower frequencies." However, it is well known that the mixing and shock components radiate noise over the same frequency range

and no method has been proposed in the past to identify the levels of the mixing noise at the higher frequencies. Figure 9 also indicates that when the shock is not very strong, as for the $M = 1.24$ case, the total noise is only ~3 dB higher than the mixing noise over a wide Strouhal number range of ~2.0–10.0. Figure 10 shows the two extracted components and the total noise for the $M = 1.24$ case at 70 deg. The mixing noise component has the same spectral level as the broadband shock-associated noise in this frequency regime, contrary to the past belief that this component is important only at the lower frequencies ("to the left of the peak"). Interestingly, this radiation angle is within an angular range where the shock noise is dominant and the mixing noise levels are low. The observation that at the higher frequencies, the mixing noise component is comparable to shock-associated noise from moderately imperfectly expanded heated jets of practical importance is surprising and somewhat unexpected. Figure 11 shows another example of the two extracted components for the $M = 1.38$ case at 70 deg. The dominance of the shock-associated noise at the higher frequencies is clearly evident for this higher Mach number case.

Figure 12 shows normalized spectra at 90 deg for the same heated case with $T_t/T_a = 3.2$, both for subsonic and supersonic Mach numbers. The nozzle diameter for this case is 1.5 in., whereas it was 2.45 in. for the spectra shown in Fig. 9. Because the effect of the nozzle size is removed in the normalization process, it does not matter what nozzle is used; however, the Strouhal number range is different for the smaller nozzle. This particular nozzle size is chosen in this figure to illustrate the point that the Strouhal number range can be extended by testing nozzles of different diameters in the construction of the normalized spectra denoted by the symbols. Figure 12 indicates that the identified velocity exponent provides an excellent spectral collapse for all subsonic Mach numbers and that the mixing noise level for the $M = 1.24$ case is identical to the normalized spectra up to a Strouhal number of ~0.5. At higher Strouhal numbers, the contribution of shock-associated noise can be identified easily. It is trivial now to carry out the subtraction of the mixing noise component from the total noise and extract the shock component. Figure 13 shows a further example at an angle of 110 deg, with $T_t/T_a = 2.7$. As seen for the previous cases, a velocity exponent of 6.72 is seen to collapse the data very well for this jet temperature and angle. Note that the mixing noise component is dominant up to a Strouhal number of 1.0 for this angle and temperature ratio.

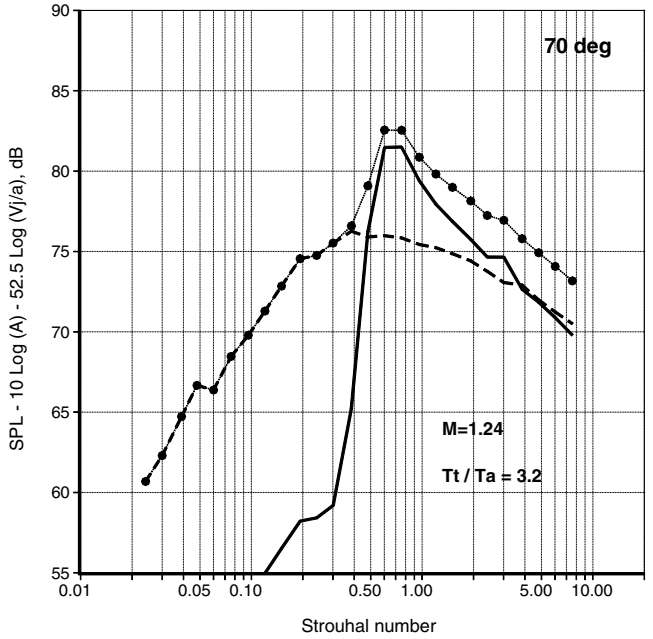

Fig. 10 Extracted components of turbulent mixing noise and broadband shock-associated noise from total measured noise. $M = 1.24$, $T_t/T_a = 3.2$, angle = 70°. Solid: shock noise; dashed: mixing noise; symbols and dotted line: total noise.

Attention is drawn to the different velocity exponents used in these three examples to collapse the data at different angles and jet temperatures. This study and Viswanathan [15] explicitly recognize and bring out the fact that the velocity exponent is strongly dependent on the radiation angle and the jet temperature ratio. As such, these two studies represent a marked departure from all the past approaches that relied on the acoustic analogy and the assumption of a dominant V^8 effect somewhat modified by additional V^4 or V^6 dependence to account for the presumed changes in source strength due to the appearance of dipoles for heated jets, and other effects such as convective amplification, Doppler correction for frequency, etc. All these approaches fail to provide satisfactory scaling laws. The velocity exponent for a fixed temperature ratio at a particular angle is obtained from the OASPL; there is no guarantee that there would be

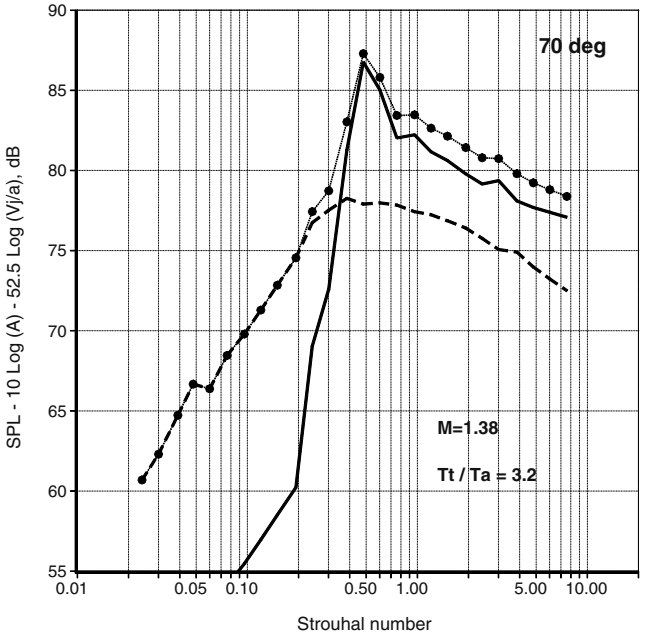

Fig. 11 Extracted components of turbulent mixing noise and broadband shock-associated noise from total measured noise. $M = 1.38$, $T_t/T_a = 3.2$, angle = 70°. Solid: shock noise; dashed: mixing noise; symbols and dotted line: total noise.

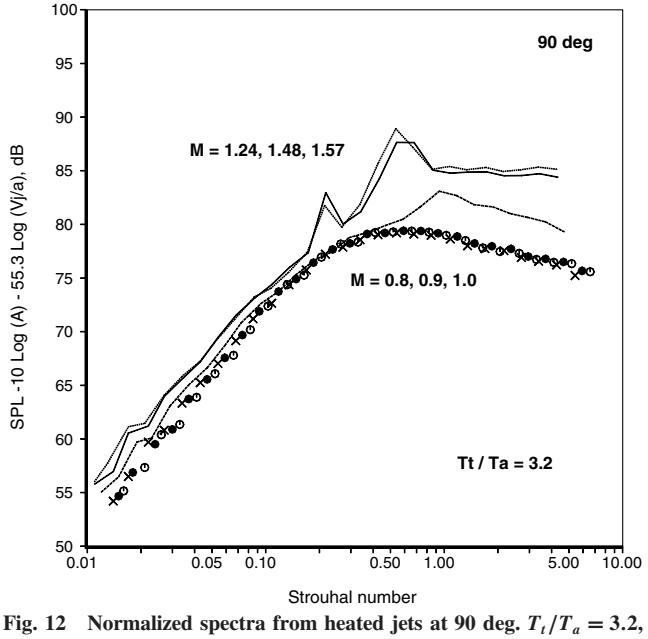

Fig. 12 Normalized spectra from heated jets at 90 deg. $T_t/T_a = 3.2$, $D = 1.5$ in. Symbols: subsonic Mach numbers; lines: supersonic Mach numbers. Velocity exponent $n = 5.53$.

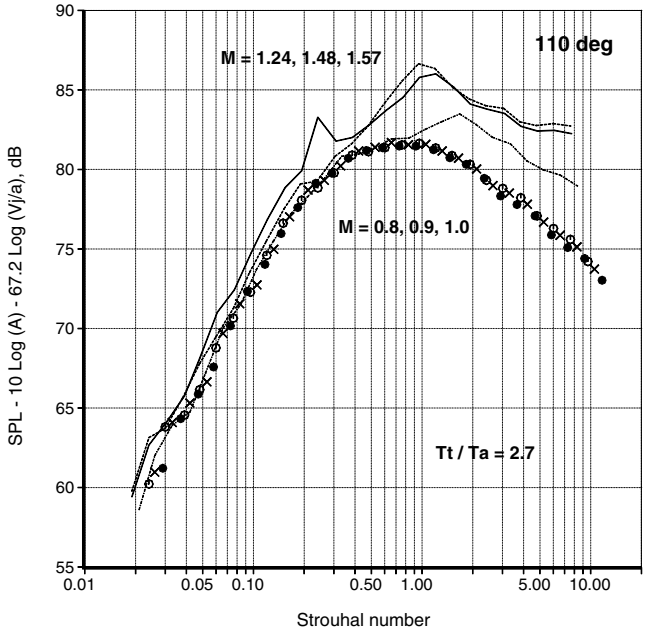

Fig. 13 Normalized spectra from heated jets at 110 deg. $T_t/T_a = 2.7$, $D = 1.5$ in. Symbols: subsonic Mach numbers; lines: supersonic Mach numbers. Velocity exponent $n = 6.72$.

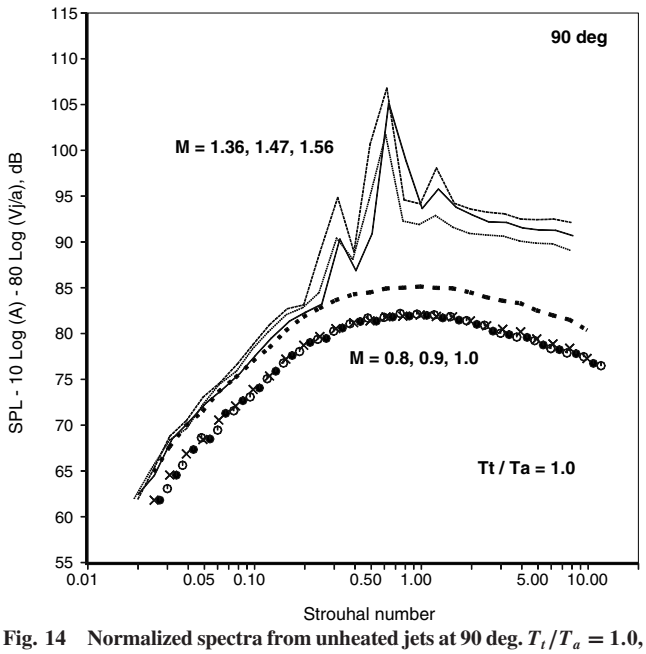

Fig. 14 Normalized spectra from unheated jets at 90 deg. $T_t/T_a = 1.0$, $D = 1.5$ in. Symbols: subsonic Mach numbers; lines: supersonic Mach numbers. Velocity exponent $n = 8.1$.

spectral collapse at all frequencies. In fact, additional factors and empiricism were introduced in the past to obtain collapse at different Strouhal numbers. The biggest difference here is the functional form chosen, where the velocity exponent, rather than the multiplicative functions, depends on the temperature ratio. It is clear from the examples shown above that this particular formulation successfully collapses the data at all frequencies, which is the goal of the scaling methodology. Additional results and discussion are provided in Sec. V.

Typical examples for unheated jets are now presented. Figure 14 shows a similar plot, with normalized spectra at 90 deg; it so happens that the velocity exponent has a value of ~8.0 at this angle. It was pointed out that this nozzle ($D = 1.5$ in.) generates intense screech tones, especially at unheated conditions, see Figs. 6 and 8. The amplitude of the screech tones is ~25 dB even for the $M = 1.24$ jet and it is well known that strong screech tones are common in unheated jets. It is readily apparent that there is significant amplification of the turbulent mixing noise, as evidenced by an increase of ~3 dB over the normalized subsonic spectra at the lower Strouhal numbers. Similar levels of amplification of the turbulent mixing noise have been observed in the experiments on unheated jets at NASA Langley and have been reported in Figs. 17 and 18 in Tam et al. [20]. Therefore, the turbulent mixing noise levels as given by the collapsed spectra from subsonic jets (without the amplification due to screech) must be adjusted, as symbolically shown by the thick dashed line, which represents the normalized spectral shape moved up to higher sound pressure levels. The levels of the shock-associated noise are more than ~8 dB at the higher frequencies over the mixing noise levels for these unheated jets at the higher Mach numbers. For the sake of information, it is noted that at a lower Mach number of 1.24 (not shown), the shock noise is 5^+ dB more than the mixing noise for Strouhal numbers greater than 0.4.

The narrowband spectra at an aft angle of 145 deg are examined in Fig. 15 for this unheated case. An exponent of 9.64 is seen to collapse the subsonic spectra, denoted by the dark and light gray lines; spectra for only two subsonic Mach numbers and one supersonic Mach number are shown so as not to clutter the plot. There is a strong screech tone with amplitude of ~17 dB at this angle, with a resultant amplification of ~5 dB at the spectral peak. Thus, the presence of strong screech tones could amplify substantially the turbulent mixing noise as already noted. This problem is severe for unheated jets as seen in Figs. 14 and 15, but not a major issue for heated jets as seen in Fig. 9b. For the heated supersonic jet at a Mach number of 1.24, the

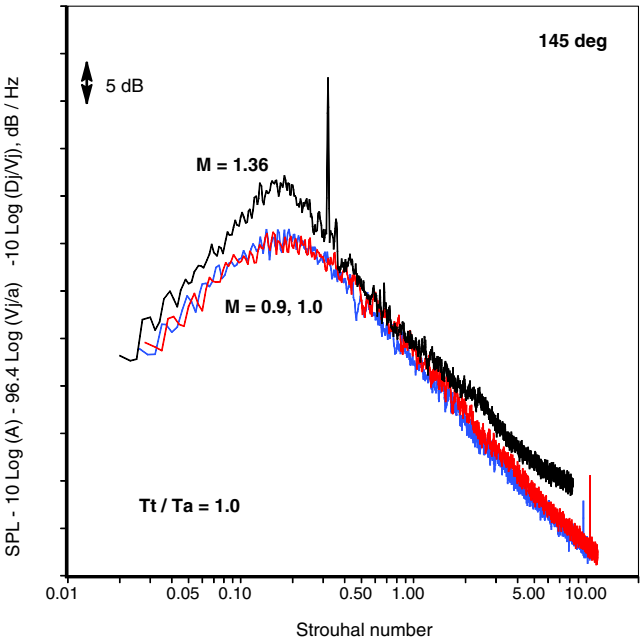

Fig. 15 Normalized spectra from unheated jets at 145 deg. $T_t/T_a = 1.0$, $D = 1.5$ in. Red (light gray): $M = 0.9$; blue (dark gray): $M = 1.0$; black: $M = 1.36$. Velocity exponent $n = 9.64$.

screech tones are entirely absent or barely discernible above the broadband shock-associated noise, see Fig. 6. For this Mach number, there is excellent agreement of the turbulent mixing noise with those for subsonic jets, as demonstrated clearly in Figs. 9a, 9b, 12, and 13. It is clear that one would have to make a distinction between jets with and without strong screech tones. The robustness of the current approach for identifying the turbulent mixing noise and extracting the two broadband components has been demonstrated with the above examples. It is obvious that the use of data normalization and scaling of spectra represent a superior method for accomplishing the above objective and removes the guesswork associated with other ad hoc approaches.

The velocity exponents for all the temperature ratios at all the angles are presented in Fig. 16. These values change slightly,

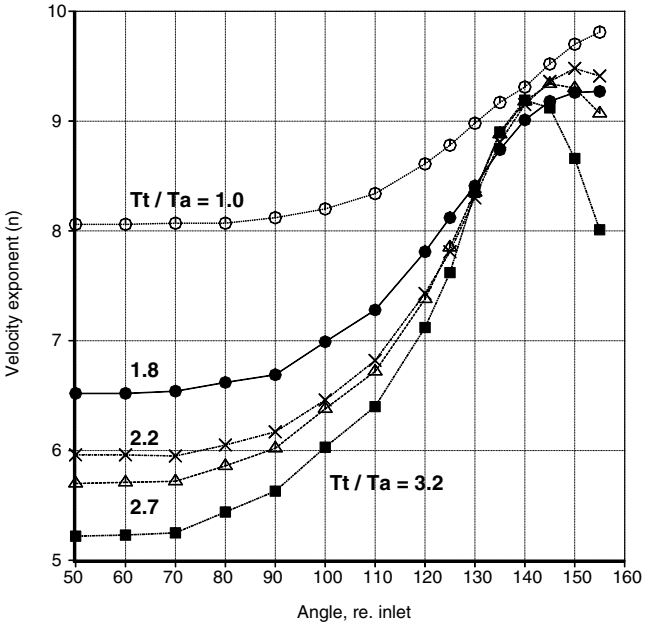

Fig. 16 Velocity exponent for various angles and jet stagnation temperature ratios.

depending on the data set and the number of test points used. However, the trends remain the same. There are several notable features: at the lower polar angles, there is a substantial drop in the value of the exponent as the jet temperature ratio is progressively increased, from ~8.0 for the unheated case to ~5.2 for the highest temperature ratio of 3.2. Further, the curves are quite flat in the forward quadrant for all T_t/T_a. Proceeding aft, the values start to increase, with the highest value of ~9.8 reached for the unheated jet at 155 deg. At an angle of 130 deg, all the heated jets have the same value for the velocity exponent. At further aft angles, the effect of jet temperature is minor, with the values of the velocity exponents more or less the same for all the temperature ratios, heated and unheated. That is, in the peak radiation sector, the effect of jet temperature on the velocity exponent is weak and the radiated noise depends only on (V_j/a). Now, in the computation of the OAPWL, the OASPL in the peak angles would play a major role. As seen in the directivity of OASPL in Fig. 2 in Viswanathan [29], for example, the peak angular sector would contribute the most energy to the sound power. Perhaps it should not be surprising then that the velocity exponent for OAPWL approaches a value of 8 as the jet temperature is increased and has only a weak dependence on temperature, as seen in Fig. 4. Viswanathan [15] also showed that the power spectra from highly heated jets with $T_t/T_a = 3.2$ and at several Mach numbers can be collapsed with the velocity exponent of eight; see Figs. 26 and 27 in the above reference.

V. Implications for Modeling

There is no complete theory for jet noise that captures the experimentally observed spectral trends at all radiation angles. As noted in Sec. III.B, a variety of formulations have been proposed for the noise intensity at 90 deg. At other radiation angles, the spectral shape is modified to account for effects due to source convection and flow/acoustics interaction. The theoretical directivity factor, as per Lighthill [21] and later modifications introduced by Ffowcs-Williams [30], is typically of the form

$$D(\theta) = [(1 - M_c \cos\theta)^2 + \alpha^2 M_c^2]^{-5/2}$$

In the above expression, M_c is the convective Mach number usually assumed to be ~65% to ~70% of the acoustic Mach number (V_j/a) and α is an empirical constant with a value of ~0.3. Lush [31] initially, and later Tanna [32] among others, investigated the validity of the theoretical directivity against their experimental measurements and found that the predicted variations were quite different from experimental data. In an effort to establish the correct velocity dependence Tanna [32] also attempted different powers of the Doppler factor, a downstream location for the noise source, different assumed values for M_c and α, etc. However, none of these approaches, with any combination of M_c, α, and the value for the exponent (−3 to −9 instead of −5), provided satisfactory results for the OASPL directivity or the collapse of the entire spectra.

The current formulation is examined over a wide range of angles, particularly in the aft quadrant. We concentrate on three temperature ratios of 1.0, 1.8, and 3.2; that is, the jet temperature is increased by ~80% each time. Table 1 provides the jet operating conditions for the test points considered. The static temperature ratio and the corresponding velocity ratio are grouped along with the stagnation temperature ratio. In the following analysis, only the subcritical pressure ratios are considered, since convergent nozzles have been tested. Note that the static temperature ratio (T_j/T_a) varies ~15%–~13.5% for the subcritical pressure ratios. Attention is drawn to a more important parametric variation of (V_j/a): the ranges for the three temperature ratios are (0.287–0.912), (0.386–1.226) and (0.516–1.643), respectively. That is, there is significant overlap of the velocity ratios, with the jet velocities at the higher NPR for the lower temperature ratios being higher than those at the lower NPR for the higher temperature jets.

The normalized spectra for various test points at 90 deg are examined first in Fig. 17 in which the appropriate values of the velocity exponent from Fig. 16 are used. The normalized spectra for the heated jets are virtually identical. Viswanathan [15] showed that the spectral shapes at the lower radiation angles have a universal shape for unheated and heated jets at all jet velocities, provided the Reynolds number is above a critical value. Figure 18 shows the normalized spectra at 125 deg for two temperature ratios of 1.0 and 1.8, denoted by numbers and symbols, respectively. The normalized spectra form two different families of curves. For the heated jets, the spectra from the two lowest velocity cases $(V_j/a = 0.386$ and $0.536)$ are also shown, denoted by the dark circles and the + sign. The spectrum at $(V_j/a = 0.536)$ is slightly contaminated by rig noise; at the lowest velocity, the levels are higher by ~3 dB indicating a higher level of contamination. However, the spectral shapes conform to those at higher velocities. That is, the spectral shape for a given temperature ratio has a unique shape regardless of jet velocity. This point is further emphasized in Figs. 19 and 20, where the normalized spectra for the three temperature ratios are depicted at 125 and

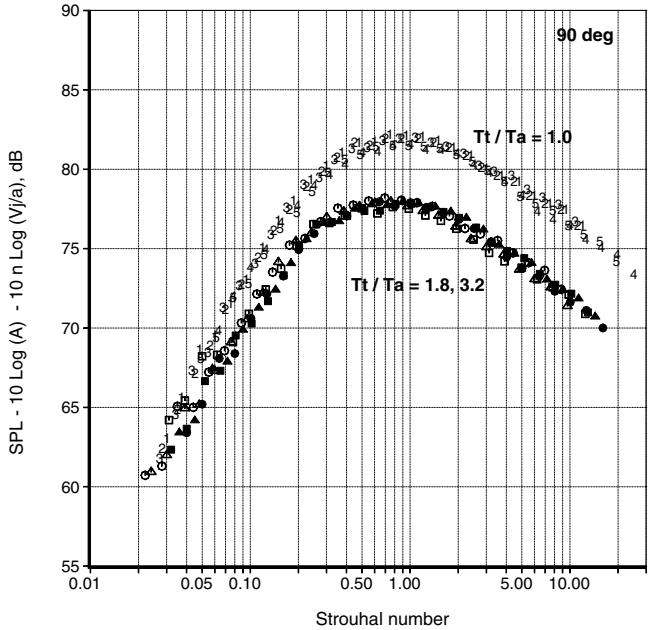

Fig. 17 Normalized spectra from jets at different velocities at 90 deg. Numbers: $T_t/T_a = 1.0$; open symbols: $T_t/T_a = 1.8$; closed symbols: $T_t/T_a = 3.2$.

Table 1 Test conditions at three temperature ratios.

NPR	T_t/T_a	T_j/T_a	V_j/a	T_t/T_a	T_j/T_a	V_j/a	T_t/T_a	T_j/T_a	V_j/a
1.06	1	0.983	0.287	1.8	1.771	0.386	3.2	3.153	0.516
1.12	1	0.968	0.399	1.8	1.744	0.536	3.2	3.109	0.717
1.19	1	0.952	0.492	1.8	1.715	0.661	3.2	3.061	0.884
1.28	1	0.932	0.584	1.8	1.681	0.784	3.2	3.005	1.049
1.39	1	0.910	0.670	1.8	1.642	0.900	3.2	2.942	1.205
1.52	1	0.887	0.751	1.8	1.602	1.009	3.2	2.876	1.351
1.69	1	0.861	0.834	1.8	1.556	1.122	3.2	2.799	1.502
1.89	1	0.834	0.912	1.8	1.508	1.226	3.2	2.721	1.643
2.50	1	0.770	1.073	1.8	1.395	1.444	3.2	2.533	1.938
3.00	1	0.731	1.161	1.8	1.326	1.562	3.2	2.418	2.098
3.50	1	0.699	1.227	1.8	1.270	1.651	3.2	2.325	2.220
4.00	1	0.673	1.280	1.8	1.224	1.722	3.2	2.247	2.317

145 deg, respectively. It is readily evident that there are three distinct families of curves, each with a unique shape, for all jet velocities within that group. Attention is also drawn to the use of the Strouhal number without the Doppler correction for frequency $[f^*(1 - M_c \cos(\theta))]$ on the x axis. See Sec. III.E in Viswanathan [19] for more details.

It is well established that the spectral shape of the turbulent mixing noise has a smooth parabolic shape at lower angles, with a gentle rise in levels with frequency up to the spectral peak followed by a gentle roll-off at the higher frequencies. At angles close to the jet axis, the spectral shape has a narrower peak, with a sharp rise followed by a sharp roll-off. For a gradual progression in spectral shape with angle, see Figs. 18 and 19 in Viswanathan [29] for example. Various reasons have been attributed to the change in spectral shape with angle: flow/acoustic interactions or contributions from the large scale turbulent structures being dominant at aft angles. In all of these explanations, the shape change is associated only with jet velocity. The equation for directivity, for example, relies on the convective Mach number M_c, which is a function of jet velocity alone. As already noted, an examination of Table 1 indicates that the jet velocity $(V_j/a = 0.912)$ for the unheated jet at a NPR of 1.89 is higher than the lowest five test points at a temperature ratio of 1.8 and the lowest three points at a temperature ratio of 3.2. Yet, the spectral shape has a narrower peak for the lower velocity jets at higher temperature in Figs. 19 and 20.

These figures indicate that the spectral shape at a particular aft angle is controlled more by the temperature ratio than the velocity ratio. This is a surprising result and the strong influence of the temperature ratio on spectral shape at aft angles has never been recognized in any prior study. It is also clear now why the directivity factors based on velocity alone fail to predict the observed trends. The evidence presented in this section and the excellent collapse of the spectra over the entire frequency range at all the angles, confirm that the temperature ratio as well as the velocity ratio are indeed the two independent parameters that control jet noise. The above analyses and the results allow the following new scaling formulation for the mixing noise spectra at any angle:

$$\mathrm{SPL}\,(\theta, \mathrm{St}) = f\left(\frac{T_t}{T_a}, n\right), \qquad n = n\left(\theta, \frac{T_t}{T_a}\right)$$

The excellent collapse of the spectra demonstrated at the various jet operating conditions further attests to the high quality of the data published by the author in several papers. Once the correct independent parameters are recognized, a single velocity exponent collapses the entire spectra over the measured frequency range of 200 Hz–80,000 Hz. This spectral collapse obviates the need for developing a separate theory, with its own set of assumptions and adjustable coefficients, for the low-frequency regime, the midfrequency regime, the high-frequency regime, etc., at a particular angle as was done in the past studies. Viswanathan [14,15] showed that the acoustic measurements from most of the facilities are contaminated by rig noise over a wide range of higher frequencies. As shown in these two references, the level of contamination is a

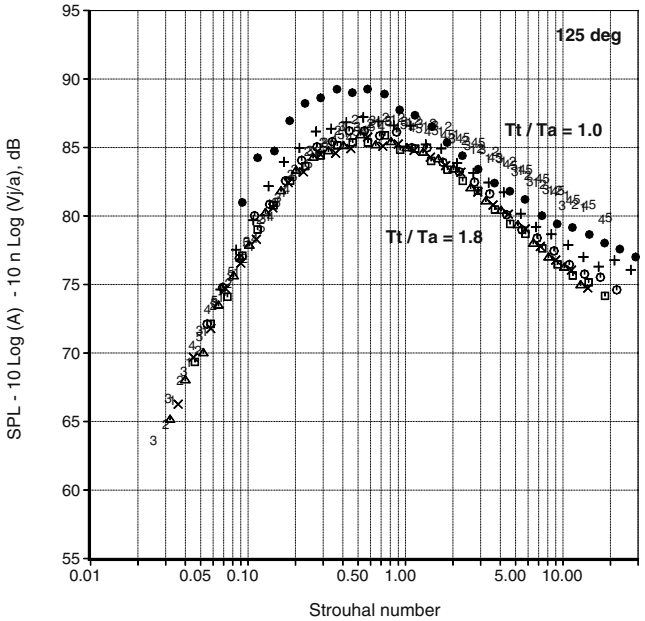

Fig. 18 Normalized spectra from jets at different velocities at 125 deg. Numbers: $T_t/T_a = 1.0$; symbols: $T_t/T_a = 1.8$; +: $(V_j/a) = 0.536$; ●: $(V_j/a) = 0.386$.

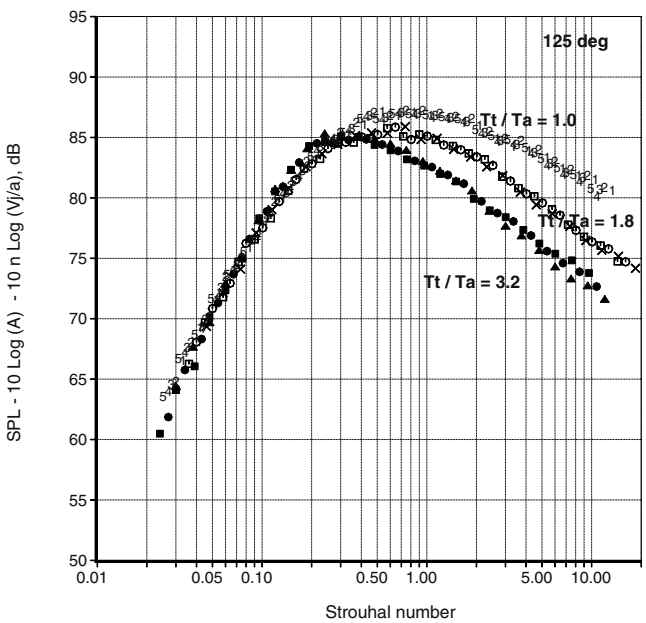

Fig. 19 Normalized spectra from jets at different velocities at 125 deg. Numbers: $T_t/T_a = 1.0$; open symbols: $T_t/T_a = 1.8$; closed symbols: $T_t/T_a = 3.2$.

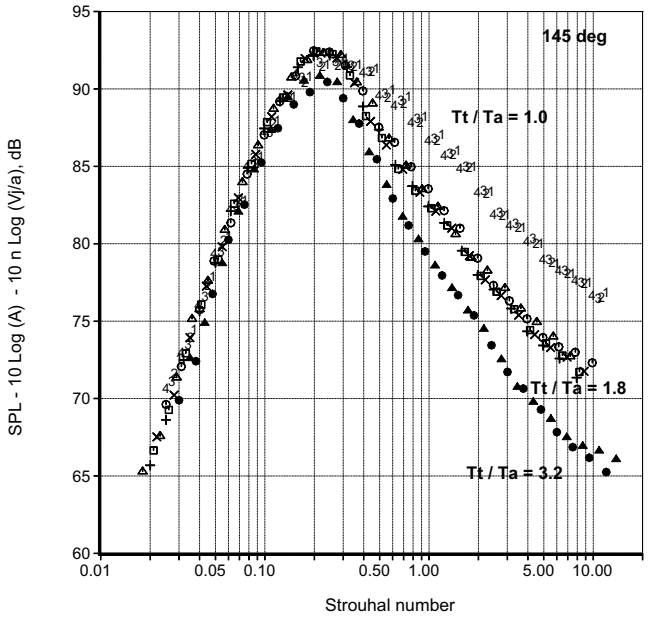

Fig. 20 Normalized spectra from jets at different velocities at 145 deg. Numbers: $T_t/T_a = 1.0$; open symbols: $T_t/T_a = 1.8$; closed symbols: $T_t/T_a = 3.2$.

strong function of the jet operating conditions (M and T_t/T_a) and varies with the radiation angle as well, with the effect of rig noise being more pronounced at the lower angles. Typically, the rig noise is stronger for unheated jets and is of less consequence for heated jets. If one were to assess the effect of heating the jet at fixed jet velocity, for example, the contribution from the rig noise could decrease as the jet temperature is increased progressively. The spectral shapes being influenced by varying levels of rig noise could yield trends that might potentially be misinterpreted as a real effect, thereby initiating the search for a suitable theory or an explanation. Thus, incorrect or nonphysical effects could be ascribed as being due to some flow variation because of bad data. It is hoped that the scaling laws developed here serve to spur new ideas or theories for jet noise.

VI. Stagnation Versus Static Temperature Ratio

In the scaling formulation, the jet stagnation temperature ratio has been shown to yield excellent spectral collapse. The question remains whether a choice of the static temperature ratio (T_j/T_a) would work equally well. In the test matrix (see Table 1 for a subset) the stagnation temperature was held constant and the static temperature was allowed to be dictated by the jet Mach number. Tanna [32] chose to hold the static temperature constant, while allowing the stagnation temperature to vary; see Fig. 1 in Tanna [32] for his test matrix. As such, within each test matrix one can only choose the particular parameter that was held constant.

To verify whether the static temperature ratio would also collapse the spectra with the new scaling formulation proposed here, the following exercise has been carried out. Sample spectra from Tanna et al. [33] were examined. An electronic database of Tanna et al. [33] is not available to the author; hence, only a few spectra were typed from Tanna et al. [33]. Viswanathan [15] showed that the unheated jet spectra in Tanna's database are contaminated by rig noise over a wide range of high frequencies even at higher jet velocities; see Fig. 5 and associated discussions on pages 46–47 and 68–71 in Viswanathan [15]. Therefore, only heated jets at a high static temperature ratio of 2.857 have been considered. Table 2 shows the test conditions, at the highest five (V_j/a) at this (T_j/T_a); the five lower velocity cases were discarded because of issues with data quality.

Normalized spectra from four of these test points at two different angles of 90 and 120 deg are shown in Figs. 21 and 22, respectively. There is reasonably good collapse of spectra, except for the scatter at the higher frequencies at 120 deg in Fig. 22. It should be noted

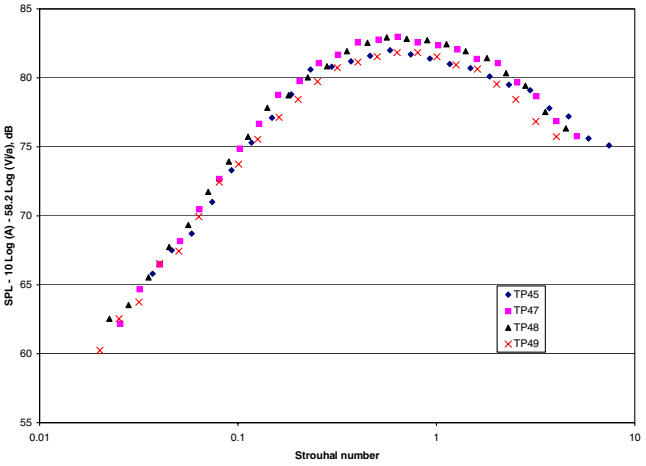

Fig. 21 Normalized spectra at 90 deg from heated jets at constant static temperature ratio of 2.857. Velocity exponent $n = 5.82$. Data from Tanna et al. [33].

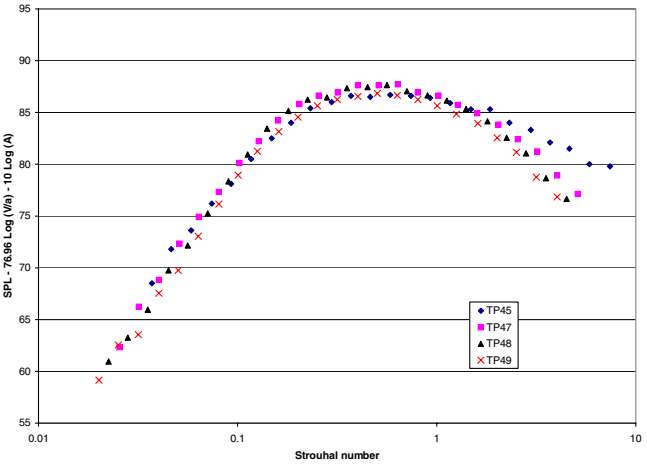

Fig. 22 Normalized spectra at 120 deg from heated jets at constant static temperature ratio of 2.857. Velocity exponent $n = 7.7$. Data from Tanna et al. [33].

Table 2 Subset of Tanna's test matrix.

TPN	NPR	T_j/T_a	T_t/T_a	V_j/a
45	1.159	2.857	2.968	0.8
46	1.205	2.857	2.997	0.9
47	1.355	2.857	3.086	1.16
48	1.483	2.857	3.158	1.33
49	1.621	2.857	3.229	1.48

though, that the spectral collapse is not as tight as seen in the previous figures with the current data and that the variation in the stagnation temperature ratio is only ~8% for the five cases considered. However, the collapse of data with the current scaling laws is far superior to those with other scaling formulations with the same database of Tanna et al. [33]; see Fig. 2 in Morfey et al. [26] or Fig. 12 in Tanna et al. [25]. It has not been verified that the overall power levels scale better with static temperature ratios, as shown with stagnation temperature ratios in Fig. 4: it would take a tedious amount of work to create an electronic database from Tanna et al. [33]. Hence, based on the limited investigation above, it is fair to say that the static temperature ratio would likely be inferior to the stagnation temperature ratio as the independent parameter. Making the velocity exponent dependent on the temperature ratio, either

stagnation or static, still represents a better approach for scaling jet noise spectra.

The practical uses of the scaling methodology developed here are obvious. An accurate empirical prediction method is a natural by-product. Further, the normalized or scaled spectra can be used to check data quality. At angles close to the jet axis, extra care is needed to collapse spectra and one has to account for nonlinear propagation effects. These issues and the applications of the scaling laws will be reported elsewhere.

VII. Conclusions

A new methodology for identifying the turbulent mixing noise component in the measured spectra from jets that contain shocks has been developed. The methodology is based on a high-fidelity experimental aeroacoustic database created by the author. The framework adopted is founded on developing scaling laws for jet noise spectra at different radiation angles. Implicit in this approach is the recognition that the jet sound power (or OAPWL) does not follow exactly the eighth-power velocity law, but has a weak dependence on jet stagnation temperature ratio. Similarly, the variation of noise intensity (or OASPL) with jet velocity at every radiation angle is a function of the jet stagnation temperature ratio. Thus, the jet temperature ratio is established as an important controlling parameter. The noise characteristics of unheated and heated jets at every radiation angle can therefore be described in terms of two independent parameters: the total temperature ratio (T_t/T_a) and the velocity ratio (V_j/a). The velocity exponent for scaling jet noise is then defined uniquely for each angle and temperature ratio. The explicit identification of these three parameters for characterizing the behavior of jet noise sets this study apart from past approaches, and yields superior scaling laws.

The velocity exponent, for every angle and temperature ratio, has been calculated from a thorough analysis of the comprehensive database. Excellent collapse of the turbulent mixing noise spectra is demonstrated for a variety of angles and temperature ratios with the computed velocity exponents, thus validating the scaling methodology. Furthermore, the excellent quality of the acoustic data is highlighted once again with the perfect collapse of the spectra over the entire measured frequency range of 200 Hz–80,000 Hz from nozzles of different diameters. Thus, additional confirmation has been provided for the assertion that it is possible to acquire high-quality data up to 80 KHz in model tests.

Strong screech tones could amplify the turbulent mixing noise. This problem is more severe for unheated jets and is of lesser consequence for highly heated jets. The scaling methodology provides a measure of the amplification of the turbulent mixing noise by screech tones. For moderately imperfectly expanded heated supersonic jets, the mixing noise component has the same spectral level as the shock-associated noise, over a wide range of higher frequencies. This new finding is contrary to the conventional belief that the mixing noise is important only at the lower frequencies to the left of the screech tone or the broadband peak of the shock-associated noise.

References

[1] Harper-Bourne, M., and Fisher, M. J., "The Noise from Shock Waves in Supersonic Jets," AGARD AGARD-CP-131, 1973, pp. 1–13.

[2] Tanna, H. K., "An Experimental Study of Jet Noise. Part 2: Shock Associated Noise," *Journal of Sound and Vibration*, Vol. 50, No. 3, 1977, pp. 429–444.

[3] Seiner, J. M., and Norum, T. D., "Experiments on Shock Associated Noise of Supersonic Jets," AIAA Paper 79-1526, 1979.

[4] Seiner, J. M., and Norum, T. D., "Aerodynamic Aspects of Shock Containing Jet Plumes," AIAA Paper 80-0965, 1980.

[5] Norum, T. D., and Seiner, J. M., "Measurements of Static Pressure and Far Field Acoustics of Shock-Containing Supersonic Jets," NASA TM 84521, 1982.

[6] Norum, T. D., and Seiner, J. M., "Broadband Shock Noise from Supersonic Jets," *AIAA Journal*, Vol. 20, No. 1, 1982, pp. 68–73.

[7] Tam, C. K. W., and Tanna, H. K., "Shock Associated Noise of Supersonic Jets from Convergent-Divergent Nozzles," *Journal of Sound and Vibration*, Vol. 81, No. 3, 1982, pp. 337–358.

[8] Seiner, J. M., "Advances in High Speed Jet Aeroacoustics," AIAA Paper 84-2275, 1984.

[9] Seiner, J. M., and Yu, J. C., "Acoustic Near-Field Properties Associated with Broadband Shock Noise," *AIAA Journal*, Vol. 22, No. 9, 1984, pp. 1207–1215.

[10] Yamamoto, K., Brausch, J. F., Janardan, B. A., Hoerst, D. J., Price, A. O., and Knott, P. R., "Experimental Investigation of Shock-Cell Noise Reduction for Single-Stream Nozzles in Simulated Flight," *Test Nozzles and Acoustic Data, Comprehensive Data Report*, Vol. 1, NACA CR-168234, May 1984.

[11] Tam, C. K. W., "Stochastic Model Theory of Broadband Shock Associated Noise from Supersonic Jets," *Journal of Sound and Vibration*, Vol. 116, No. 2, 1987, pp. 265–302.

[12] Tam, C. K. W., "Jet Noise Generated by Large-Scale Coherent Motion," *Aeroacoustics of Flight Vehicles: Theory and Practice: Noise Sources*, edited by H. H. Hubbard, Vol. 1, NASA, Washington, DC, 1991, pp. 311–390; RP-1258.

[13] Anon., "Gas Turbine Jet Exhaust Noise Prediction," SAE ARP876, Revision D, 1994.

[14] Viswanathan, K., "Jet Aeroacoustic Testing: Issues and Implications," *AIAA Journal*, Vol. 41, No. 9, 2003, pp. 1674–1689.

[15] Viswanathan, K., "Aeroacoustics of Hot Jets," *Journal of Fluid Mechanics*, Vol. 516, October 2004, pp. 39–82.

[16] Viswanathan, K., and Clark, L. T., "Effect of Nozzle Internal Contour on Jet Aeroacoustics," *International Journal of Aeroacoustics*, Vol. 3, No. 2, 2004, pp. 103–135.

[17] Viswanathan, K., "Instrumentation Considerations for Accurate Jet Noise Measurements," *AIAA Journal*, Vol. 44, No. 6, 2006, pp. 1137–1149.

[18] Shields, F. D., and Bass, H. E., "Atmospheric Absorption of High Frequency Noise and Application to Fractional-Octave Band," NASA NASA-CR 2760, 1977.

[19] Viswanathan, K., "Does a Model Scale Nozzle Emit the Same Jet Noise as a Jet Engine?" *AIAA Journal* (to be published).

[20] Tam, C. K. W., Golebiowski, M., and Seiner, J. M., "On the Two Components of Turbulent Mixing Noise from Supersonic Jets," AIAA Paper 96-1716, 1996.

[21] Lighthill, M. J., "On Sound Generated Aerodynamically: 1. General Theory," *Proceedings of the Royal Society of London, Series A: Mathematical and Physical Sciences*, Vol. 211, 1952, pp. 564–581.

[22] Fisher, M. J., Lush, P. A., and Harper Bourne, M., "Jet Noise," *Journal of Sound and Vibration*, Vol. 28, No. 3, 1973, pp. 563–585.

[23] Morfey, C. L., "Amplification of Aerodynamic Noise by Convected Flow Inhomogeneities," *Journal of Sound and Vibration*, Vol. 31, No. 2, 1973, pp. 391–397.

[24] Lilley, G. M., "Aerodynamic Noise," Noise Mechanisms, AGARD AGARD-CP-131, 1974, pp. 13.1–13.12.

[25] Tanna, H. K., Dean, P. D., and Fisher, M. J., "The Influence of Temperature on Shock-Free Supersonic Jet Noise," *Journal of Sound and Vibration*, Vol. 39, No. 4, 1975, pp. 429–460.

[26] Morfey, C. L., Szewczyk, V. M., and Tester, B. J., "New Scaling Laws for Hot and Cold Jet Mixing Noise Based on a Geometric Acoustics Model," *Journal of Sound and Vibration*, Vol. 61, No. 2, 1978, pp. 255–292.

[27] Goldstein, M. E., "An Exact Form of Lilley's Equation with a Velocity Quadrupole/Temperature Dipole Source Term," *Journal of Fluid Mechanics*, Vol. 443, 2001, pp. 231–236.

[28] Goldstein, M. E., "A Unified Approach to Some Recent Developments in Jet Noise Theory," *International Journal of Aeroacoustics*, Vol. 1, 2002, pp. 1–16.

[29] Viswanathan, K., "Nozzle Shaping for Reduction of Jet Noise from Single Jets," *AIAA Journal*, Vol. 43, No. 5, May 2005, pp. 1008–1022.

[30] Ffowcs-Williams, "The Noise from Turbulence Convected at High Speed," *Philosophical Transactions of the Royal Society*, Vol. A255, 1963, pp. 469–503.

[31] Lush, P. A., "Measurements of Subsonic Jet Noise and Comparison with Theory," *Journal of Fluid Mechanics*, Vol. 46, Pt. 3, 1971, pp. 477–500.

[32] Tanna, H. K., "An Experimental Study of Jet Noise. Part 1: Turbulent Mixing Noise," *Journal of Sound and Vibration*, Vol. 50, No. 3, 1977, pp. 405–428.

[33] Tanna, H. K., Dean, P. D., and Burrin, R. H., "The Generation and Radiation of Supersonic Jet Noise: Turbulent Mixing Noise," Vol. 3, U. S. Air Force Aero Propulsion Laboratory, AFAPL-TR-76-65, 1976.

D. Gaitonde
Associate Editor